ELSEVIER

Thermochimica Acta 304/305 (1997) 369–378

thermochimica acta

Modulated differential scanning calorimetry study of blends of poly(butylene terephthalate) with polycarbonate

Y.Y. Cheng[1], M. V. Brillhart[2], Peggy Cebe*

Department of Physics and Astronomy, Science and Technology Center, Tufts University, Medford, MA 02155 , USA

Received 25 August 1996; accepted 21 May 1997

Abstract

Modulated differential scanning calorimetry (MDSC) was used to study the glass-transition relaxation behavior in blends of poly(butylene terephthalate) (PBT), a semicrystalline polymer, with polycarbonate (PC), an amorphous polymer. Using a temperature-modulated differential scanning calorimeter (TM-DSC), a sinusoidal temperature oscillation was superimposed upon the underlying linear temperature ramp. The reversing, total, and non-reversing heat flow curves were then analyzed. We examined the efficacy of modulated differential scanning calorimeter (MDSC) to extract glass transitions (T_g) when these were covered over by rapid cold crystallization occurring in the same temperature range.

Blends were available in PBT/PC compositions of 80/20 and 40/60, and with high and low molecular weight, M_w, designated 'H' or 'L', respectively. Samples of very low initial crystallinity were prepared by rapid quenching from the melt. These samples crystallized immediately during the MDSC scan producing complex exothermic peaks when the scanning temperature increased over T_g. All blends exhibited a lower glass transition assigned to the PBT-rich phase. The upper glass transition, assigned to the PC-rich phase, was never observed in 80H/20L, 80L/20L, or 40L/60L. This suggests that PC-L has better miscibility with amorphous PBT, while producing a very broad, indistinct glass transition in the PC-rich phase. The Fox equation was used to determine the mass fraction composition of the two phases, and confirms that better miscibility is achieved when low molecular weight components are blended.

Higher crystalline blends were prepared by melt crystallization. The size of the glass-transition step was greatly reduced in the melt crystallized blends compared to the quenched blends. Nonetheless, MDSC was used successfully to observe dual glass transitions at intermediate temperatures between the T_gs of the homopolymers for all melt crystallized blends, except 80L/20L. Analysis of the lower T_g indicates better amorphous phase miscibility in blends with PBT-L and PC-L; analysis of the upper T_g indicates better amorphous phase miscibility in blends with PBT-L. © 1997 Elsevier Science B.V.

Keywords: Crystallization; Glass transition; Modulated differential scanning calorimetry; Polymer blends

1. Introduction

Thermal analysis has been an important analytical tool for the study of binary polymer blends [1–11]. In blends of two non-crystallizable polymers, differential scanning calorimetry has been used very effectively to determine the glass-transition relaxation behavior. Fox developed an empirical equation to estimate the fraction of blend components contributing to the strength of the glass transitions in partially miscible systems [12]. If the binary blend has one or both polymers crystallizable, then additional thermal events may be studied. These include the crystallization and melting

*Corresponding author

[1]Present Address: F2, No.25, LN295, Fushing S. Rd., Taipei, Taiwan.

[2]Present address: Hewlett Packard Electronics Devel. Ctr., Palo Alto, CA 94304.

PII S0040-6031(97)00202-5

behavior, degree of crystallinity, and effect of crystals on the glass transitions in the blend.

Recently, the technique of modulated differential scanning calorimetry (MDSC), also referred to as temperature-modulated DSC, has become available and provides capabilities not found in conventional DSC [13–16]. A sinusoidal temperature profile is superimposed on the underlying linear heating ramp so that the temperature at any time, t, is given by:

$$T(t) = T_0 + \beta t + A_T(\sin\omega t) \quad (1)$$

where T_0 is the initial temperature, β the underlying heating rate, A_T the amplitude of modulation, and ω the angular frequency in radians/s. ω is related to the chosen oscillation period, p, by $\omega = 2\pi/p$. In Eq. (1), we have used the notation suggested by Reading [16]. Excellent reviews of this technique can be found in several recent references [13],[15–18].

Temperature oscillation allows the separation of the heat flow into the total heat flow, a response to the average linear heating rate, and a second cyclic component related to the heat capacity effect [16]. In the MDSC instrument commercially available from TA Instruments, the second heat flow related to the heat capacity is termed the 'reversing' heat flow. Processes that are reversible on the time scale of the experiment, such as glass-transition relaxations, will appear in the reversing heat-flow curve. Other events which are not reversible, such as cold crystallization and enthalpic relaxation, are separately displayed in the 'non-reversing' heat-flow curve. This is found by direct subtraction of the total and reversing heat-flow curves. The ability of MDSC to separate out multiple glass transitions, hidden under complex thermal events, is one advantage of this new thermal analytical approach. In several recent reports, MDSC has been applied to homopolymers and blend systems [19–23]. In the work of Hourston et al. [19–22], MDSC was applied to the study of the glass transition of homopolymers, and miscibility and glass-transition behavior of amorphous/amorphous blends.

Here, we report results of thermal analysis of binary crystallizable blends of poly(butylene terephthalate) (PBT), with bisphenol A polycarbonate (PC). PBT is known to crystallize rapidly, but is somewhat brittle in spite of its low glass-transition temperature. PC does not normally crystallize and has a much higher glass-transition temperature, near 155°C. One of the rationales for the use of crystalline/amorphous blends is the improvement of specific properties. In PBT/PC, PBT imparts solvent resistance to the blend, while PC improves the use temperature and toughness. This blend system has been studied by our group and others [7],[24–31] using dynamic mechanical relaxation, small angle X-ray scattering and thermal analysis. Several groups studied the phase behavior and determined that PBT/PC exhibits upper critical solution temperature UCST-type of phase diagram [24,25,29]. Recently, using techniques of thermal analysis, and electron microscopy [29,30], the PBT and PC domains have been imaged and their morphology in relation to the phase behavior suggested.

In this study we were particularly interested in blends which were quenched so that their initial degree of crystallinity was very low. PBT homopolymer itself crystallizes rapidly, so that PBT/PC blends will immediately undergo 'cold crystallization' when they are heated above T_g during the MDSC scan. This blend system thus provides an extreme test of the usefulness of MDSC for the separation of a glass transition hidden under the cold crystallization exotherm. Once the glass transitions are resolved, we can apply the Fox equation to determine the relative composition of the phases in this partially miscible blend system.

2. Experimental

PBT and PC homopolymer and blends were obtained from General Electric in a variety of molecular weights and blend compositions. The blends were stabilized with phosphoric acid to prevent transesterification reaction [32]. All materials were melted only for short times (2 min), and at a relatively low temperature (250°C), to inhibit further transreaction [30,31,33]. In this work, we report results from high (H) and low (L) molecular weight PBT (M_w = 108000 or 65000g/mol) blended with high or low molecular weight PC (M_w = 36500 or 19100g/mol).

Quenched samples were prepared by compression molding thin films at 250°C between ferrotypes plates covered with Kapton™ film to ensure easy removal of the blend films. Pressure was applied to the blend pellets for ca. 2 min, and the films were quenched in an

ice water bath. The quenched films were very slightly hazy, including existence of some initial degree of crystallinity.

Using the quenched samples as starting materials, some films were melt crystallized in a Mettler FP80 hot stage. Films were again melted at 250°C for 2 min, then cooled at 20°C min^{-1} to 205°C where they were held for 1 h. Films were cooled to room temperature inside the hot stage at a cooling rate of 3°C/min.

Modulated differential scanning calorimetry (MDSC) was performed at a scanning rate of 3°C/min. using a TA Instruments 2920 DSC in the modulated mode. Exothermic response is shown as upward deflection in all heat-flow plots. Temperature was calibrated using indium, and baseline was calibrated as in conventional DSC using two empty aluminum pans. Either sapphire or high density polyethylene was used to calibrate heat capacity. The sample mass was between (5–8) mg. The empty reference pan was matched in mass to the sample pan to within 0.05 mg.

For MDSC on the quenched samples, a modulation amplitude of either 0.32°C (or 1.0°C) and a temperature modulation period of either 40 s (or 60 s) were used. These small modulation amplitude and period were chosen whenever samples were heated through the melting transition. This choice was made so that the heating rate was always above zero, i.e. almost no cooling occurred during the scanning process. Helium was used as a heat transfer gas at a flow rate of ca. 30 ml min^{-1}. The heat of fusion of perfectly crystalline PBT, $\Delta H_f^0 = 142$ J/g [34], was used to calculate the initial degree of crystallinity in the quenched samples.

To explore the glass-transition region in some quenched and melt crystallized samples, a larger oscillation amplitude of 1°C was chosen with 60 s period, and nitrogen purge gas at a flow rate of 30 ml/min.

The samples tested span a wide range in composition and thermal behavior, especially in their cold crystallization kinetics. Except in a few instances, we chose to keep the MDSC parameters exactly the same among the samples to facilitate direct comparison. This resulted in an occasional inferior deconvolution of the reversing heat-flow curve (due to insufficient number of cycles in the oscillation) in samples with rapid kinetics.

3. Results and discussion

3.1. MDSC on quenched samples

Quenching was used to create samples with low initial degrees of crystallinity. Because of the tendency for the PBT to crystallize rapidly, it was very difficult to achieve an amorphous quenched sample. All homopolymers and blends were slightly hazy, though not at all brittle. This indicated the presence of a small amount of crystallinity in the samples prior to MDSC scanning. The ability of the MDSC to detect the glass transitions when these were possibly hidden underneath cold crystallization and enthalpic relaxation events was explored.

Fig. 1a shows the modulated heat flow (upper curve) and the derivative of the modulated tempera-

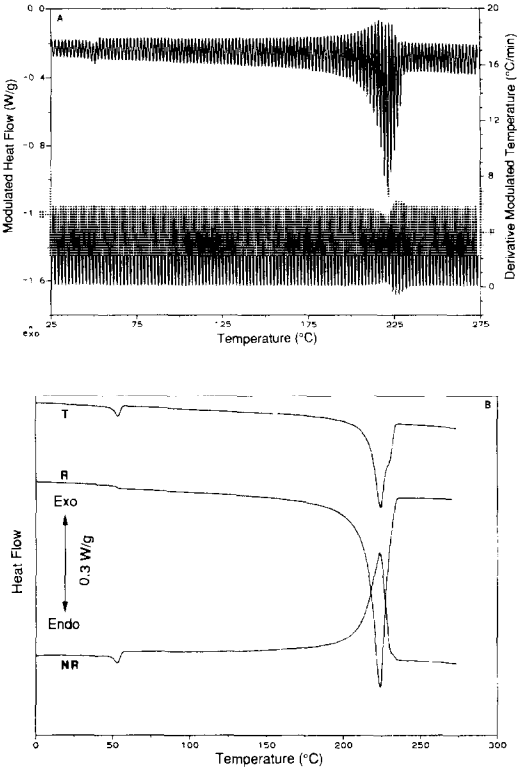

Fig. 1. MDSC results vs. temperature for quenched PBT-L (100L/0) scanned at 3°C/min, with oscillations of ±0.32°C every 40 s. (a) – Modulated heat flow (upper curve) and derivative of modulated temperature (lower curve); and (b) – Total (*T*), reversing (*R*), and non-reversing (*NR*) heat flows.

ture, or modulated heating rate (lower curve), for homopolymer PBT-L(100/0) quenched from the melt. The sinusoidal oscillations in the heating rate and heat flow are apparent. Nearly over the entire scan, the heating rate is above zero, indicating that the sample is heated only, and not cooled. Only near the major melting event, just above 220°C, does the heating rate briefly dip below zero. Fig. 1b shows the total (*T*), reversing (*R*), and non-reversing (*NR*) heat flows derived from the raw data shown in Fig. 1a. The total heat flow (*T*) gives the same level information as conventional DSC and reflects the sum of all the thermal events experienced during the scan. The *T* curve shows a small minimum near 53°C, followed immediately by an exothermic step up reflecting the immediate cold crystallization when temperature rises above T_g. At higher temperatures, a major endothermic event occurs at 224°C which reveals a shoulder on the high temperature side. The *R* curve shows a distinct glass transition at 53°C, followed by the melting endotherm at 224°C. Subtraction of *R* from *T* gives the non-reversing curve. *NR* shows an enthalpic relaxation at ca. 53°C and an exothermic step just above, followed by a major exotherm at 223°C. From Fig. 1b, we see that the *R* curve depicts the PBT-L glass transition clearly, whereas from the *T* curve (similar to conventional DSC) the glass-transition temperature would be difficult to determine.

Some of the quenched blends exhibited two glass transitions, indicative of liquid–liquid phase separation into a PBT-rich phase with lower T_g, and a PC-rich phase with higher T_g. An example is 40H/60L, and the total (*T*), reversing (*R*), and non-reversing (*NR*) heat flows for this blend are shown in Fig. 2. The *T* curve has an endothermic relaxation at 51°C, followed by a broad exotherm. A second sharper exotherm is seen at 145°C, followed by the major melting endotherm at 222°C. The *R* curve shows the two glass transitions very clearly, at 50°C and 113°C, respectively. Then follows the melting endotherm at 223°C. Again, it is very clear that the determination of the glass-transition temperatures would be difficult, if not impossible, using only the total heat flow curve. In this sample, it appears that crystallization can occur in either of the two phases, when the glass-transition temperature of that phase is exceeded. Finally, the *NR* curve shows an endothermic relaxation peak at 51°C, one broad and one sharper exotherm, at 65°C and 145°C, respectively. There is a broad exotherm in the vicinity of the melting region, a feature seen in the *NR* curves of all samples. The interpretation of this exothermic feature in *NR* curves is presently being investigated [19,35].

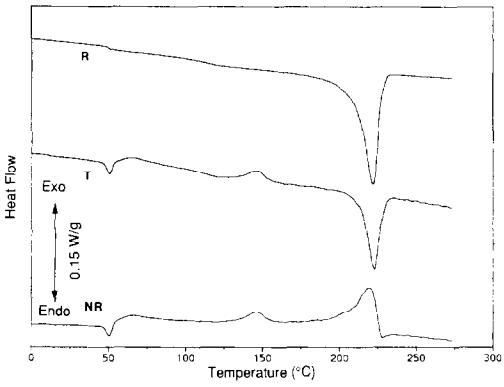

Fig. 2. MDSC results for quenched PBT/PC 40H/60L blends scanned at 3°C/min, with oscillations of ±0.32°C every 40 s. Total (*T*), reversing (*R*), and non-reversing (*NR*) heat flows vs. temperature.

Other blends, especially those with lower molecular weight PC (such as 40L/60L) showed only a single glass transition. Fig. 3(a) shows the total (*T*), reversing (*R*), and non-reversing (*NR*) heat flows for 40L/60L quenched blend scanned through the melting transition. In the *T* curve, a relaxation is seen near the glass-transition region at 65°C, followed by a large crystallization exotherm at ca. 111°C and, finally, the melting endotherm is seen at 223°C. In the *R* curve, the lower glass transition is seen at 76°C, followed by the melting endotherm. No upper glass transition can be seen. The non-reversing heat flow shows a small relaxation peak at ca. 65°C followed by a crystallization exotherm at 111°C.

Another sample of 40L/60L was scanned only to 175°C using a larger oscillation amplitude of 1°C/min. This scan is shown in Fig. 3(b). In spite of a baseline fluctuation in the *R* curve (at the crystallization temperature), the glass-transition step is very clear, and only a single glass transition can be seen. The 40L/60L sample was then cooled and rescanned, and the results are shown in Fig. 3(c). All three curves are quite featureless up to about 110°C. At that temperature, *T* and *R* shows a glass transition at 126°C. No evidence of the lower T_g can be seen. Apparently, the crystals forming at 111°C during the first scan were formed in the PBT-rich phase

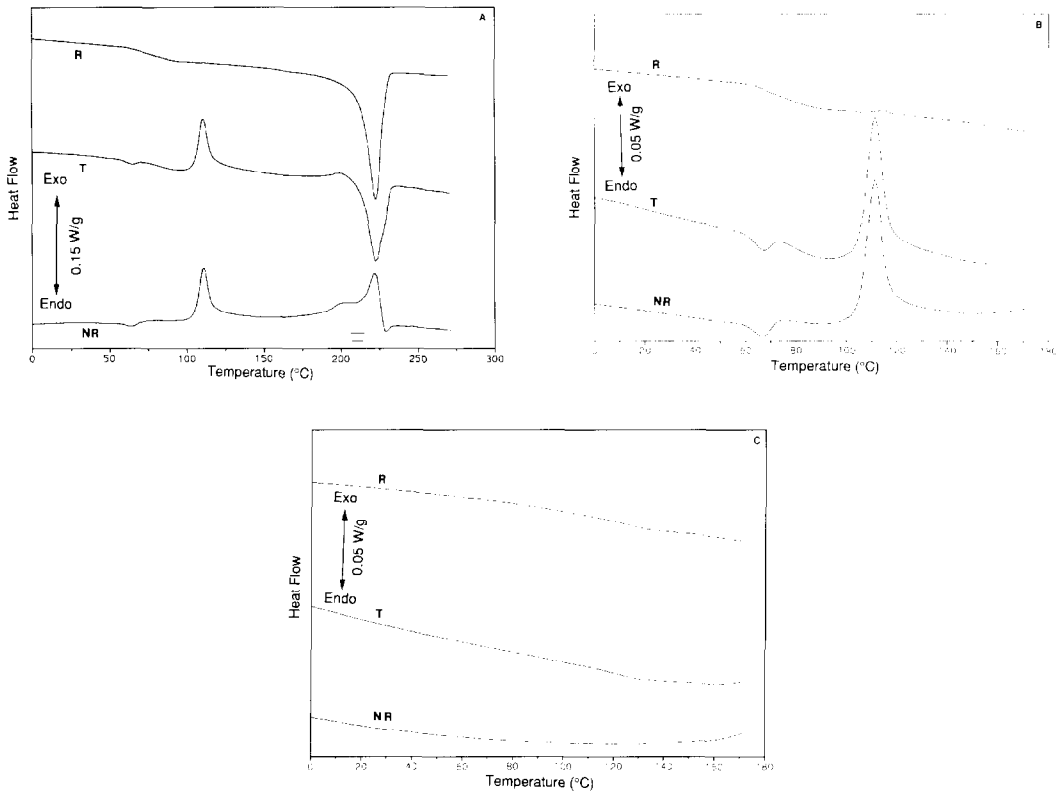

Fig. 3. MDSC results for PBT/PC 40L/60L blends scanned at 3°C/min. Total (*T*), reversing (*R*) and non-reversing (*NR*) heat flows vs. temperature. (a) – Quenched sample with oscillations of ±32°C every 40 s; (b) – Quenched sample with oscillations of ±1.0°C every 60 s; and (c) – Second scan of the sample shown in (b).

and constrained the remaining amorphous chains so that they no longer could exhibit a glass transition under these scanning conditions. This is similar to PBT homopolymer, in which crystals create a large fraction of the rigid amorphous phase [32] as indicated by the decrease in the heat capacity step. As PBT crystallizes in the 40L/60L blend, it forms pockets of PBT-rich material, that are surrounded by a depletion layer rich in PC. This PC-rich portion now could cause the glass transition at higher temperatures, as seen in Fig. 3(c).

Very complex exothermic behavior of quenched 40L/60H blends can be seen in Fig. 4 showing the total (*T*), reversing (*R*), and non-reversing (*NR*) heat flows up to 175°C. The *T* curve shows an endothermic relaxation at the lower T_g. Then a broad exothermic response follows at 53°C, with several sharper exothermic features superimposed at 73°C and 140°C. The behavior of this blend presents a severe

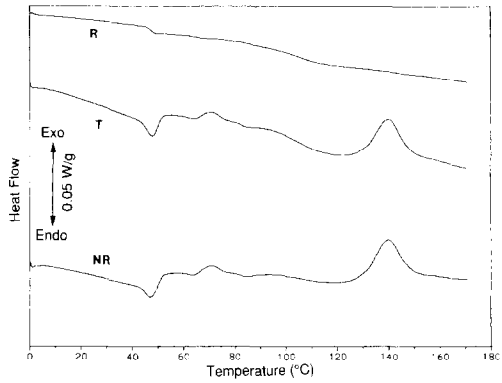

Fig. 4. MDSC results for PBT/PC 40L/60L blends scanned at 3°C/min, with oscillations of ±1.0°C every 60 s. Total (*T*), reversing (*R*), and non-reversing (*NR*) heat flows vs. temperature.

test of the ability of MDSC to separate the glass transitions which are hidden by the crystallization exotherms. In the *R* curve, the lower T_g is clearly

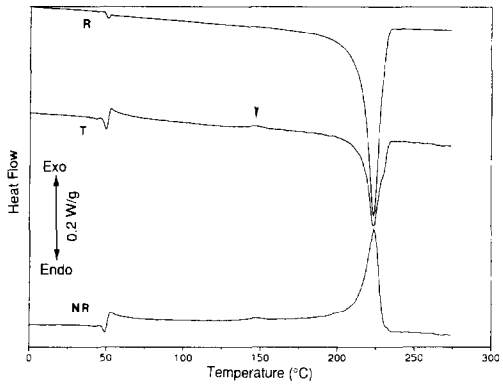

Fig. 5. MDSC results for quenched PBT/PC 80L/20H blends scanned at 3°C/min, with oscillations of ±0.32°C every 40 s. Total (*T*), reversing (*R*), and non-reversing (*NR*) heat flows vs. temperature.

seen at 48°C, while the broader upper T_g is seen at 102°C.

Occasionally, the upper T_g was so weak that it could not be seen even using MDSC analysis. An example is shown in Fig. 5 for 80L/20H quenched blend. The reversing heat flow curve exhibits only a single-glass transition occurring at 49°C (with a small superimposed relaxation endotherm) followed by the major melting endotherm at 224°C. However, both *T* and *NR* curves in Fig. 5 show exothermic heat flow peaks. One occurs immediately above the low T_g at ca. 53°C, the second is very weak but distinguishable and marked with an arrow at 150°C. The last occurs in NR at 223°C. Here, it is not surprising that the second glass-transition temperature is not observable, since the fraction of PC in this blend is low. Nonetheless, the small exothermic peak in the *T* and *NR* curves near 150°C suggests that further crystallization in the PC-rich phase may be occurring when the temperature is increased sufficiently to provide the necessary mobility for the PBT chains in the PC-rich phase to crystallize.

All the glass-transition temperatures of quenched samples are listed in the first two columns of Table 1. A lower T_g from the PBT-rich phase is seen in all compositions and molecular weight combinations. An effect of molecular on the lower T_g is seen in the 40L/60L. These blends have the lower T_g shifted up in temperature 40°. Other 40/60 blends have lower T_g up-shifted by only 10°. This indicates that in the PBT-rich phase of 40/60 blends, PBT-L has better miscibility with PC-L than does PBT-H.

An upper T_g was not seen in several 80/20 blends, due to the low overall fraction of PC, small fraction of the PC-rich phase and better miscibility between PC-L and amorphous PBT. Blends containing PC-H had upper T_g reduced by 30–40°. Blends 80/20 with PC-L never displayed an upper T_g in the quenched sample form. In 40/60 blends having much larger fraction of PC, an upper T_g was not seen in the

Table 1
Glass-transition temperature for quenched or melt crystallized PBT/PC blends from modulated differential scanning calorimetry

Sample[a]	Quenched		Melt crystallized	
	lower T_g(°C)	upper T_g (°C)	lower T_g(°C)	upper T_g (°C)
100H/0	41	n [c]	38	n [c]
100L/0	53	n [c]	38	n [c]
80H/20H	48	122	48	129
80H/20L	47	— [b]	49	128
80L/20H	46	110	47	129
80L/20L	49	— [b]	48	— [b]
40H/60H	49	123	57	138
40H/60l	50	113	52	131
40L/60H	48	102	57	132
40L/60L	76	— [b]	58	122
0/100H	n [c]	152	n [c]	152
0/100L	n [c]	141	n [c]	141

[a] PBT and blends were melt crystallized at 205°C for 1.0 h.
[b] Not observed.
[c] Not applicable.

composition L/L. These results taken together suggest that PC-L has much better miscibility with PBT than does PC-H. The L/L composition causes a much broader and flatter glass transition. The relaxation-time distribution of the amorphous chains in the PC-rich phase is broadened sufficiently by the existence of PBT-L so that the T_g is not seen in MDSC analysis.

3.2. Initial degree of crystallinity

The quenching process was designed to produce a low initial degree of crystallinity. To determine the initial crystallinity, we used the area under the T curve for samples heated through the melting transition. The extrapolation of the high-temperature (melt) part of the curves back to lower temperature was used to determine the areas, ΔH^T or ΔH^R, under the T or R curves, respectively. These areas are listed in the first two columns of Table 2 for all the quenched blends and homopolymers. Since the cold crystallization sometimes begins at a temperature within the glass transition step, we did not use the same low-temperature point on the R and T curves for the determination of the area. Instead, to calculate the area under the R curves, we chose a starting point which was from 5–20° (depending upon the breadth of the transition) above the inflection point in the T_g step. This choice reflects the observation that polymer crystals do not melt at their formation temperature, but melt above the crystallization temperature by 10–15°.

Table 2
MDSC heats of reaction from total (T) and reversing (R) heat flow curves, and initial and partial mass fraction crystallinities for quenched homopolymers and PBT/PC blends

PBT/PC	ΔH^T/ J/g	ΔH^R/ J/g	$\chi_{c,t}$ [a]	$\chi_{c,p}$ [b]
100H/0	27.8	165.6	.20	.20
100L/0	27.8	184.3	.20	.20
80H/20H	12.1	130.6	.09	.11
80H/20L	14.4	128.2	.10	.13
80L/20H	19.9	139.8	.14	.18
80L/20L	10.2	133.8	.07	.09
40H/60H	5.2	67.2	.04	.09
40H/60L	4.4	51.9	.03	.08
40L/6H	8.3	57.1	.06	.15
40L/60L	−.1	56.6	—	—

[a] Initial total crystallinity calculated from Eq. (2a).
[b] Initial partial crystallinity calculated from Eq. (2b), with $f = 1.0$, 0.8, 0.4 for 100/0, 80/20 and 40/60, respectively.

Using the T-curve area determined in this way, we derive the initial total, or partial, degree of crystallinity for the quenched samples from:

$$\chi_{c,t} = (\Delta H^T)/(\Delta H_f^0) \quad (2a)$$

$$\chi_{c,p} = (\Delta H^T)/\phi(\Delta H_f^0) \quad (2b)$$

where ΔH^T is the measured endotherm area, in J/g of samples mass, ΔH_f^0 is the heat of fusion of 100% crystalline PBT, and ϕ is the mass fraction of PBT in the blend. Total crystallinity, $\chi_{c,t}$ refers to the amount of crystals in the entire sample while partial crystallinity, $\chi_{c,p}$ refers to the amount of crystals in the PBT fraction of the sample. For homopolymer PBT, ϕ is 1.0, while for the blends it is either 0.8 or 0.4. These results are listed in the last two columns of Table 2. Initial crystallinity of quenched PBT homopolymer is 0.20. For the quenched blends, the initial crystallinity ranges from ca. 0.03 to 0.14 of the total mass fraction. Blends 80/20 had greater initial crystallinities than 40/60. The areas under the 80/20 reversing heat flow curves are about twice as large as the areas under the 40/60 reversing heat flow curves. A much large fraction of crystallinity can develop during the MDSC scan in 80/20 than in 40/60 blends.

The greatest initial partial crystallinity occurred in L/H, regardless of composition. We suggests that PBT-L crystallizes faster when blended with PC-H than it does in other formulations, so the quenching was not as effective in yielding samples of low initial crystallinity.

3.3. Melt crystallized PBT/PC blends

In homopolymer PBT, crystallization reduces the heat capacity step at the glass transition due to the formation of rigid amorphous chains [36]. Therefore, it was supposed that the melt crystallized PBT/PC blends would also have features of small amplitude. In order to explore the effects of melt crystallization on the glass-transition behavior of the PBT blends, a larger oscillation amplitude was used to increase the size of observed features.

Fig. 6(a) and (b) show a comparison of the reversing heat flow curves for quenched and melt crystallized blends. Here, in the quenched amorphous 80/20 blend (Fig. 6(b)) the glass transition is so narrow, and recrystallization so rapid, that there were not sufficient

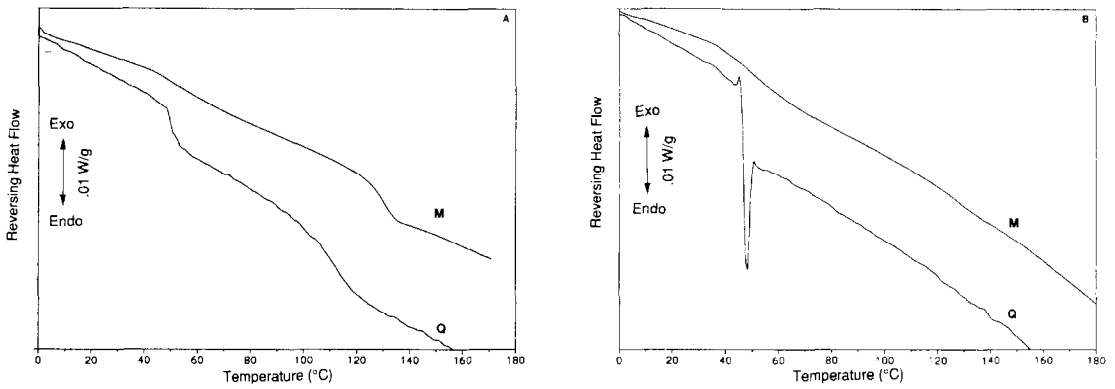

Fig. 6. MDSC reversing heat flow vs. temperature for PBT/PC blends scanned at 3°C/min. Quenched blend, *Q*, with oscillations of ±32°C every 40 s. Melt crystallized blend, *M*, with oscillations of ±1.0°C every 60 s. (a) – 40H/60L; (b) – 80H/20L

oscillations spanning the transition, and the deconvolution used to obtain the reversing curve is inferior, and results in a downward spike. Nonetheless, we may compare the behavior of this blend with its melt crystallized partner, and with the 60/40 composition shown in Fig. 6(a). These data point up the general problem associated with MDSC parameter selection whenever a series of materials with widely varying properties is to be studied.

Fig. 6(a) compares 40H/60L quenched sample, scanned with oscillation amplitude of 0.32°C, and melt crystallized sample, scanned with oscillation amplitude of 1.0°C. The effects of melt crystallization are to reduce the size – and upshift the temperature – of the lower transition. The upper T_g is also upshifted by 10–20°, and is sharper in the melt crystallized sample. This confirms our earlier suggestion that PBT crystallizes in the PC-rich phase, leaving a depletion zone rich in PC, which has T_g closer to the PC homopolymer. Glass transitions of melt crystallized blends are listed in the last two columns of Table 1. Melt crystallization has a negligible effect on the lower T_g of the 80/20 blends.

3.4. Fox analysis of phase composition

Analysis of the glass transition was performed according to the Fox equation [12], which is:

$$1/T'_{gj} = \sum_i W_{ij}/T_{gi} \qquad (3)$$

where T'_{gj} is the measured glass transition of the *j*th peak in the blend ($j = 1$, lower peak; $j = 2$, upper peak). W_{ij} is the mass fraction of the *i*th component ($i = 1$, PBT; $i = 2$, PC) in the *j*th peak, and T_{gi} is the glass transition of the *i*th homopolymer component.

The Fox analysis takes no account of the effects of degrees of crystallinity or amount of rigid amorphous phase, on the transition. Here, we make the simplifying assumption that the entire shift in the glass-transition temperature arises from the effects of blending, and not from crystallinity. This may be a reasonable assumption for the quenched blends which have low initial degree of crystallinity. Results of the Fox analysis are listed in Table 3 for the quenched blends, and in Table 4 for the melt crystallized blends.

Table 3
Mass fractions W_{ij} for PBT/PC quenched blends [a]

Blend	Mass fractions [b]			
PBT/PC	W_{11} [c]	W_{21} [c]	W_{12} [c]	W_{22} [c]
80H/20H	.88	.12	.21	.79
80H/20L	.89	.11	— [d]	— [d]
80L/20H	.91	.09	.32	.68
80L/20L	.86	.14	— [d]	— [d]
40H/60H	.87	.13	.20	.80
40H/60L	.85	.15	.22	.78
40L/60H	.88	.12	.36	.64
40L/60L	.56	.44	— [d]	— [d]

[a] Determined from Eq. (3)[12].
[b] Based on T_g results in Table 1.
[c] W_{ij} represents mass fraction of the *i*th component in the *j*th peak, normalized for each peak, where $\sum_i W_{ij} = 1$. Indexes are assigned as follows: $i = 1$ (PBT), 2(PC); $j = 1$ (lower peak). 2 (upper peak).
[d] No upper T_g was seen in this sample.

Table 4
Mass fractions W_{ij} for PBT/PC melt crystallized blends [a]

Blend	Mass Fractions [b]			
PBT/PC	W_{11} [c]	W_{21} [c]	W_{12} [c]	W_{22} [c]
80H/20H	.88	.12	.16	.84
80H/20L	.86	.14	.10	.90
80L/20H	.90	.10	.16	.84
80L/20L	.87	.13	— [d]	— [d]
40H/60H	.79	.21	.09	.91
40H/60L	.83	.17	.07	.93
40L/60H	.79	.21	.13	.87
40L/60L	.76	.24	.15	.85

[a] Determined from Eq. (3)[12].
[b] Based on T_g results in Table 2.
[c] W_{ij} represents mass fraction of the ith component in the jth peak, normalized for each peak, where $\sum_i W_{ij} = 1$. Indexes are assigned as follows: $i = 1$ (PBT), 2(PC); $j = 1$ (lower peak), 2 (upper peak).
[d] No upper T_g was seen in this sample.

In Table 3, the quenched blends show greater miscibility in the PBT-rich phase in the compositions containing L/L. The lower glass transition contains 56% PBT and 44% PC in the 40L/60L blend. Data are limited for the upper T_g. Nonetheless, better miscibility in the PC-rich phase is found in the L/H compositions than in the H/H compositions. Molecular weight plays a greater role in determining mass fractions in the upper T_g than does the overall blend composition.

Once the sample crystallizes from the melt, the fraction of PBT contributing to the upper peak, W_{12}, is reduced. Still, the greatest miscibility in the PC-rich phase occurs in blends L/L. This result suggests that melt crystallization occurs in the PC-rich phase, and leaves an amorphous layer which contains less PBT. In the 80/20 blends, the composition of the lower T_g is unaffected by melt crystallization. W_{21} is about the same for quenched and melt crystallized blends. In 40/60 blends, the lower T_g contains a greater amount of PC in the melt crystallized samples, except for 40L/60L. Crystallization within the PBT-rich phase results in a remaining amorphous layer which has relatively more PC in it.

4. Conclusions

MDSC was used to investigate the glass transition in blends of PBT with PC. Nearly all blends showed two glass transitions, indicating liquid–liquid phase separation into a PBT-rich phase, and a PC-rich phase. For 80/20 blends, the molecular weight of the components has little effect on the lower T_g in either quenched or melt crystallized samples. The upper T_g is affected most in blends containing low molecular weight PC due to the better miscibility of PC-L with amorphous PBT. Overall, miscibility is improved through the use of low molecular weight components.

In 40/60 blends, melt crystallization generally cause the lower T_g to be increased compared to the quenched blends due to an increase in the phase separation inside the amorphous regions of the PBT-rich phase (40L/60L was the exception). Crystallization of PBT in the PC-rich phase causes the upper T_g to be increased significantly after melt crystallization, leaving amorphous regions richer in PC. Crystallization of PBT can occur in either the PBT-rich or the PC-rich phase, driving both upper and lower glass transitions to higher temperatures.

Acknowledgements

This research was supported by the U.S. Army Research Office through contracts DAAH04-96-1-0009 AND DAAH04-94-G-0317. The authors thank: Dr. Mary Garbauskas and Dr. Patrick van Ende for providing the blends; Eric Che Dureiux and Leonardo Grimaldi for assistance with sample preparation; and Elizabeth Oyebode for the Fox analysis.

References

[1] T. Nishi and T.T. Wang, Macromolecules, 8 (1975) 909.
[2] T.T. Wang and T. Nishi, Macromolecules, 10 (1977) 421.
[3] P.B. Rim and J.P. Runt, Macromolecules, 17 (1984) 1520.
[4] M. Kimura, R.S. Porter and G. Salee, J. Polym. Sci., Phy. Ed., 21 (1983) 367.
[5] J. Runt and K.P. Gallagher, Polym. Commun., 32 (1991) 181.
[6] P. Huo and P. Cebe, Macromolecules, 26 (1993) 3127.
[7] Y.Y. Cheng, M. Brillhart, P. Cebe and M. Capel, J. Polym. Sci., Polym. Phys. Ed., 34 (1996) 2953.
[8] G. Crevecouer and G. Groeninckx, Macromolecules, 24 (1991) 1190.
[9] B.S. Hsiao and B. Sauer, J. Polym. Sci., Poly. Phys. Edn., 31 (1993) 901.
[10] J.P. Runt, X. Zhang, D.M. Miley, K.P. Gallagher and A. Zhang, Macromolecules, 25 (1992) 3902.

[11] J.P. Runt, D.M. Miley, X. Zhang, K.P. Gallegher, K. McFeaters and J. Fishburn, Macromolecules, 25 (1992) 1929.
[12] T.G. Fox, Bull. Am. Phys. Soc., 1 (1956) 123.
[13] M. Reading, D. Elliot and V.L. Hill, J. Thermal Anal., 40 (1993) 949.
[14] M. Reading, B. Hahn and B. Crowe, US Patent 5,244,775, 1993.
[15] M. Reading, Trends Polym. Sci., 8(1) (1993) 248.
[16] M. Reading, A. Luget and R. Wilson, Thermochim. Acta, 238 (1994) 295.
[17] B. Wunderlich, Y. Jin and A. Boller, Thermochim. Acta, 238 (1994) 277.
[18] B. Wunderlich and A. Boller, Proc. 24th American Thermal Analysis Society, San Francisco, 1995, p. 136.
[19] D.J. Hourston, M. Song, A. Hammiche, H.M. Pollock and M. Reading, Polymer, 37(2) (1996) 243.
[20] D.J. Hourston, M. Song, H.M. Pollock and A. Hammiche, Proc. 24th North American Thermal Analysis Society, San Francisco, 1995, p. 109.
[21] M. Song, A. Hammiche, H.M. Pollock, D.J. Hourston and M. Reading, Polymer, 36(17) (1995) 3313.
[22] M. Song, A. Hammiche, H.M. Pollock, D.J. Hourston and M. Reading, Polymer, 36(25) (1996) 5661.
[23] S.F. Goodkowsky, R.B. Cassel and M.P. DiVito, Proc. 24th North American Thermal Analysis Society, San Francisco, 1995, p. 130.
[24] Y.V. Konyukhova, N.P. Bessonova, S.I. Belousov, V.I. Feldman and Y.K. Godovskii, Polymer Science, 33 (1991) 2262.
[25] N. Abdeyev and A. Ye. Chalykh, Proc. Conf. 'Polymer Blends', vol. 25, 1990.
[26] J. Devaux, P. Godard and J.P. Mercier, J. Polym. Sci., Polym. Phys. Edn., 20 (1982) 1881.
[27] D. Wahrmund, D.R. Paul and J. Barlow, J. Appl. Poly. Sci., 22 (1978) 2155.
[28] J. Devaux, P. Godard and J.P. Mercier, Polym. Eng. Sci., 22 (1982) 229.
[29] D. Delimoy, B. Goffaux, J. Devaux and R. Legras, Polymer, 36(17) (1995) 3255.
[30] A. van Bennekom, Ph.D. Dissertation, University of Twente, The Netherlands, 1995.
[31] A. van Bennekom, R.J. Gaymans and J. Bussink, 1995 International Chemical Congress of Pacific Basin Societies, Honolulu HA, Dec., 1995, p. 17–22.
[32] Private correspondence with Dr. Mary Garbauskas of GE, 1996.
[33] R.S. Porter and L.H. Wang, Polymer, 33 (1992) 2019.
[34] K.H. Illers, Colloid Polym. Sci., 258 (1980) 117.
[35] W. Sichina, Proc. 24th North American Thermal Analysis Society, San Francisco, 1995, p. 123.
[36] S. Cheng, R. Pan and B. Wunderlich, Macromol. Chem., 189 (1988) 2443.